

Chain Conformation of Water-Insoluble Hyperbranched Polysaccharide from Fungus

Yongzhen Tao, Lina Zhang,* Fan Yan, and Xiaojun Wu

Department of Chemistry, Wuhan University, Wuhan 430072, China

Received March 26, 2007; Revised Manuscript Received May 2, 2007

Water-insoluble polysaccharide (TM3a), extracted from sclerotia of *Pleurotus tuber-regium*, was identified as a hyperbranched β -D-glucan from the results of one- and two-dimensional NMR and GC-MS analysis. The degree of branching of TM3a is 65.5%. TM3a was fractionated by using a non-solvent addition method into 14 fractions, and its solution properties in 0.25 M LiCl/dimethylsulfoxide (DMSO) solution were studied systematically by using static laser light scattering, dynamic light scattering, and viscometry at 25 °C. The dependences among the values of intrinsic viscosity ($[\eta]$), radius of gyration ($\langle S^2 \rangle_z^{1/2}$), and hydrodynamic radius (R_h) on weight-average molecular weight (M_w) were found as the following: $[\eta] = 0.46M_w^{0.30 \pm 0.01}$, $\langle S^2 \rangle_z^{1/2} = 4.79 \times 10^{-2}M_w^{0.43 \pm 0.04}$, and $R_h = 5.01 \times 10^{-2}M_w^{0.41 \pm 0.02}$ in the M_w range from 1.94×10^5 to 2.06×10^7 for TM3a in a 0.25 M LiCl/DMSO solution at 25 °C. The current theory of polymer solution was applied to explain the relationship among the fractal dimension, ratio of geometric to hydrodynamic radius ($\rho = \langle S^2 \rangle_z^{1/2}/R_h$), and $M_w A_2/[\eta]$ of TM3a. The results indicated that TM3a existed as a compact chain conformation with a sphere-like structure in LiCl/DMSO solution. Furthermore, by using transmission electron microscopy, we observed directly the spherical molecules with an average diameter of 23.0 ± 1.8 nm.

Introduction

The studies of fungal polysaccharides have attracted attention in the fields of biochemistry and pharmacology because of the wide varieties of their biological activity.¹ Some polysaccharides, which exhibit antitumor activities, have been obtained from the fruiting body, mycelia, or sclerotia of fungi, and they are regarded as biological response modifiers.² Interestingly, with the same chemical structure, polysaccharides being extracted from different sources display different types of chain conformations in solutions, such as single helical,³ triple helical,⁴ and flexible⁵ chain conformations for β -(1 \rightarrow 3)-D-glucan from *Auricularia auricula-judae*, *Lentinus edodes*, and *Poria cocos*, respectively. The immune stimulating effect is related to the molecular weight, branching, and chain conformation of polysaccharides to various extents.^{6,7} Triple helix lentinan exhibited a relatively high inhibition ratio against the proliferation of tumor cells, whereas the bioactivity of its single flexible chains almost disappeared. The study of the correlation between chain conformations and biological activities of polysaccharides is one of the most intriguing and challenging scientific endeavors in the 21st century.

Characterization of hyperbranched polysaccharide is more complicated than characterizing a linear polysaccharide. However, its molecular structure usually determines some specific properties, such as low viscosity and high density of chain ends at the molecular periphery, large specific surface, etc. This suggests that polysaccharides can be applied in various areas of the food industry, pharmaceuticals, surface phenomena, study of life, and materials technology.^{8–11} The periphery of hyperbranched molecules has many endgroups that can be functioned and used as sites to interact with their surroundings in a specific manner.¹² Therefore, it is very important to discover natural hyperbranched polysaccharides and to clarify

their structures and solution properties. Most of past studies have concentrated on the solution properties of synthetic hyperbranched polymers.^{13–16} The molecular characteristics of hyperbranched polysaccharide from fungi have been scarcely published. However, it is essential to understand the solution properties of hyperbranched polysaccharides for further research and biochemical or medical application of this natural biopolymer. Moreover, we have accumulated experience in characterizing molecular parameters for some biopolymers.^{17–19}

Sclerotia of *Pleurotus tuber-regium* grow in tropic and subtropical regions as an edible mushroom.²⁰ It is consumed not only for its flavor and nutritive value but also for its medicinal effects, including the treatment of asthma, smallpox, and high blood pressure.²¹ TM3a extracted from sclerotia of *Pleurotus tuber-regium*, is a water-insoluble polysaccharide, but it can be dissolved in 0.25 M LiCl/dimethylsulfoxide (DMSO). In this work, we attempted to study the chemical structure and conformation parameters of TM3a by using one- and two-dimensional NMR and GC-MS, static light scattering, dynamic light scattering, and viscometry. With applying the theory of polymer solutions, we analyzed the molecular parameters of the branched polysaccharide. Transmission electron microscopy (TEM) was used to observe the shape and size of the polymer molecules. This work provides valuable and fundamental information to further understand the chain conformation of hyperbranched polysaccharides in solution. Moreover, we hope to clarify if the current concept of polymer solutions is suitable to depict complex and natural hyperbranched polysaccharides.

Experimental Procedures

Sample Preparation. Sclerotia of *Pleurotus tuber-regium* were provided by Prof. Peter C. K. Cheung of the Department of Biology in the Chinese University of Hong Kong. Dried sclerotia powder of

* To whom correspondence should be addressed. Tel.: +86-27-87219274; fax: +86-27-68754067; e-mail: lnzhang@public.wh.hb.cn.

Pleurotus tuber-regium was defatted sequentially by using the Soxhlet extraction method with solvents of ethyl acetate and acetone for over 6 h, respectively. The residue was immersed stepwise in 0.15 M aqueous NaCl at 20, 80, and 120 °C. In each step, the mixture was stirred overnight and then was centrifuged at 9045g for 20 min to obtain a supernatant. The supernatants were labeled as TM1, TM2, and TM3, respectively. The TM3 supernatant formed two phases during the cooling process to room temperature. The centrifugation gave two types of crude polysaccharide fractions, namely, TM3a (water-insoluble) and TM3b (water-soluble). TM3a was then dissolved in 0.25 M LiCl/DMSO and was fractionated by following a non-solvent addition method. A mixture of acetone and 0.25 M LiCl/DMSO at a volume ratio of 4:1 was slowly added into the TM3a solution at 25 °C until the solution turned slightly milky. The turbid mix was warmed up to 50 °C to become transparent again. After being brought to 25 °C and standing for 12 h, the turbid solution then was centrifuged to separate into a liquid and gel phase. The gel part was removed, and the supernatant was subjected to the next step of fractionation. In this way, the TM3a sample was divided into 14 fractions and coded as F1, F2, F3, ..., through F14. Each fraction was reprecipitated by the addition of acetone, then washed with anhydrous acetone 3 times, and finally vacuum-dried to give white powder.

Characterization. An infrared spectrum (IR) of the TM3a samples was recorded with a Nicolet 170SX FT-IR spectrometer (Spectrum One, PerkinElmer Co., Madison, WI) in the range of 4000–400 cm⁻¹ using the KBr-disk method. One- and two-dimensional ¹H and ¹³C NMR measurements of TM3a were analyzed on a Mercury 600 NMR spectrometer (Varian Inc., Palo, Alto, CA) at 20 °C. TM3a was dissolved in DMSO to obtain a concentration of 50 mg/mL. Gas chromatography–mass spectrometry (GC-MS) was carried out on an Agilent 6890N GC system equipped with a capillary split/splitless injector system and a flame ionization detector on an HP-5MS capillary column (30 m × 0.32 mm × 0.25 μm) and a mass spectrometer (5973N, Agilent, Palo Alto, CA). To determine sugar composition and linkage, the polysaccharide was permethylated twice by using CH₃I and solid NaOH in DMSO as a sequential method as described.²² The methylated polysaccharide was subsequently hydrolyzed with 12 M H₂SO₄ (35 °C, 1 h) and 2 M H₂SO₄ (120 °C, 1 h) and then reduced with NaBH₄. After neutralization and removal of boric acid by evaporation with methanol, the mixture of partially methylated alditols was acetylated with acetic anhydride (Ac₂O) at 120 °C for 3 h. The resultant product was analyzed by GC-MS with the injection of 0.2 μL of a sample solution. The oven temperature was set at 150 °C and was increased by 2 °C/min to 220 °C. The detector temperature was set at 280 °C, and nitrogen was used as a carrier gas.

The intrinsic viscosity ($[\eta]$) of the TM3a fractions in 0.25 M LiCl/DMSO was measured at 25 ± 0.1 °C by using an Ubbelohde capillary viscometer. The kinetic energy correction was assumed to be negligible. Huggins and Kraemer equations were used to estimate the $[\eta]$ value by extrapolating to an infinite

dilution formulated as

$$\eta_{sp}/c = [\eta] + k'[\eta]^2c \quad (1)$$

$$(\ln \eta_r)/c = [\eta] - \beta[\eta]^2c \quad (2)$$

Both k' and β are constants for a given polymer at a given temperature in a given solvent, η_{sp}/c is the reduced specific viscosity, and $(\ln \eta_r)/c$ is the inherent viscosity.

M_w and radius of gyration ($\langle S^2 \rangle_z^{1/2}$) of the TM3a fractions in 0.25 M LiCl/DMSO were measured with a laser light scattering instrument equipped with a He–Ne laser (MALLS, $\lambda = 633$ nm; DAWN DSP, Wyatt Technology Co., Santa Barbara, CA) at multiple angles (θ) in the range from 26 to 142° at 25 °C. The basic light scattering equation is as follows

$$\frac{Kc}{R_\theta} = \frac{1}{M_w} \left(1 + \frac{16\pi^2 \langle S^2 \rangle_z \sin^2(\frac{\theta}{2})}{3\lambda^2} \right) + 2A_2c + \dots \quad (3)$$

where K is an optical constant equal to $[4\pi^2 n^2 (dn/dc)^2] / (\lambda^4 N_A)$, c is the polymer concentration in mg/mL, R_θ is the Rayleigh ratio, λ is the wavelength; n is the refractive index of the solvent; dn/dc is the refractive index increment; N_A is Avogadro's number, and A_2 is the second virial coefficient. The polysaccharide solution with desired concentrations was prepared, and optical clarification of the solution was achieved by being filtrated through a 0.2 μm pore size filter (PTFE, Puradisc 13 mm Syringe Filters, Whatman, Kent, U.K.) into a scattering cell. The refractive index increment (dn/dc) was measured with a double-beam differential refractometer (DRM-1020, Otsuka Electronics Co., Tokushima, Japan) at a wavelength of 633 nm. The dn/dc value of TM3a in 0.25 M LiCl/DMSO was 0.031 cm³ g⁻¹. Astra software V4.90.07 was utilized for data acquisition and analysis.

The hydrodynamic radii (R_h) of the samples were measured on a Zetasizer nanoparticle analyzer (Malvern Instruments Ltd., Malvern, U.K.) by using dynamic light scattering (DLS). The solutions of the TM3a polysaccharide and their fractions in 0.25 M LiCl/DMSO were prepared at a concentration of 3.0 mg/mL, and all the measurements were carried out at 25 °C.

Molecular morphology of the TM3a specimen was performed on a high-resolution transmission electron microscope (JEM-2010, JEOL, Tokyo, Japan). The objective lens raster was added to enhance the contrast, and the images were recorded by a CCD digital camera. The samples were prepared with dissolving 10 mg of TM3a in 5 mL of 0.25 M LiCl/DMSO. Each of the samples was vigorously stirred for 24 h. After purification through a 0.2 μm filter, a droplet of the sample solution was deposited on a holey carbon film, which was supported by a copper grid. A thin layer was suspended over the holes of the grid. The specimen was finally dried in air at ambient temperature and pressure and then TEM images were taken at an accelerating voltage of 200 kV.

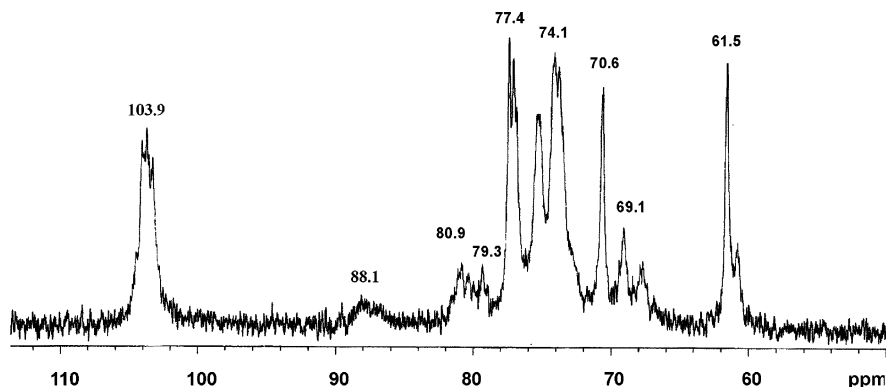


Figure 1. ¹³C NMR spectrum of TM3a in DMSO-*d*₆.

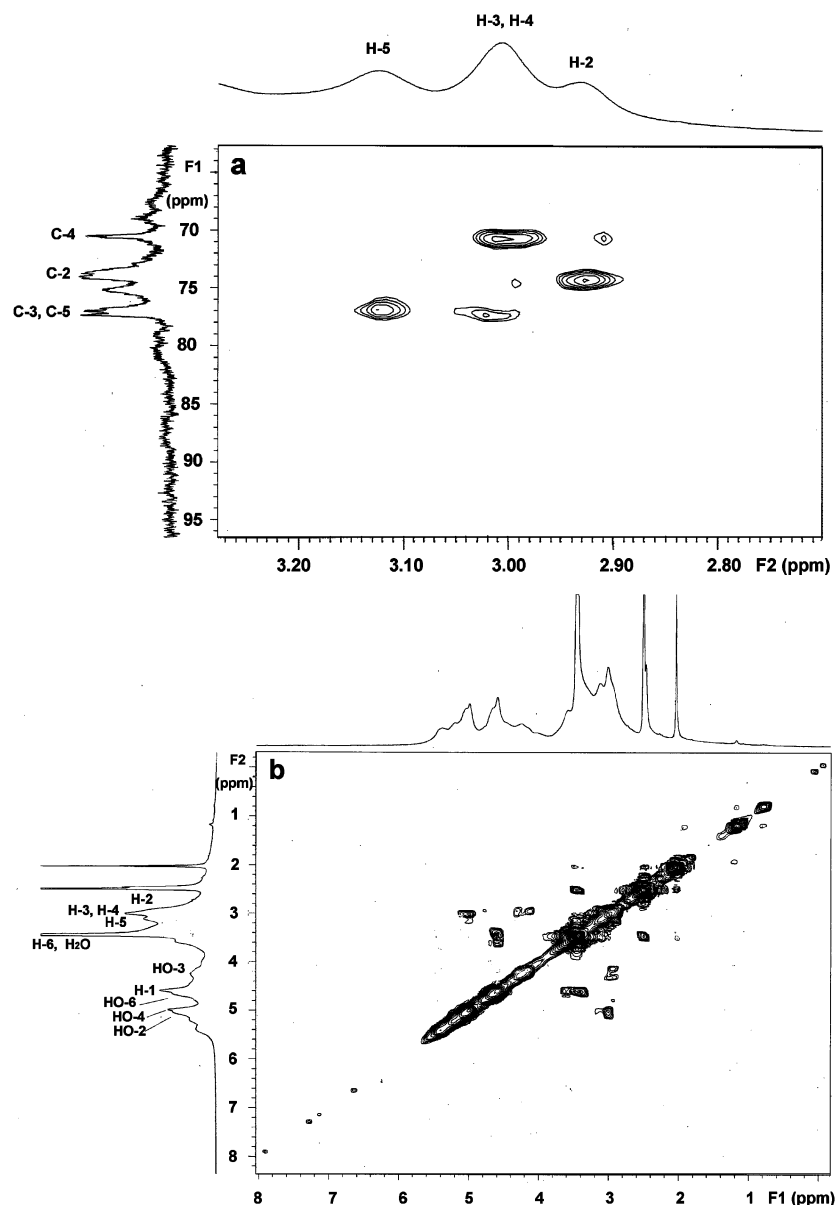


Figure 2. HMQC (a) and DQF (b) of NMR spectrum for TM3a in DMSO- d_6 at 20 °C.

Results and Discussion

Chemical Structure. IR spectrum of the TM3a samples (not shown) exhibits an absorption peak at 890 cm^{-1} , which is characteristic of the β configuration of glucan.²³ The ^{13}C NMR spectrum of TM3a in DMSO- d_6 is shown in Figure 1. The major signals were assigned to 103.9 ppm for C1, 77.4 ppm for C3 and C5, 74.1 ppm for C2, 70.6 ppm for C4, and 61.5 ppm for C6. They show similar peak positions as those of the carbons for methyl- β -D-glucopyranose.²⁴ These peaks were assigned to the carbons of the non-reducing β -D-glucopyranosyl terminals of TM3a. The result indicates that TM3a is a kind of polysaccharides having numerous terminal units and characterizes it as a hyperbranched polysaccharide as reported.²⁵ Furthermore, the signals at 88.1, 80.9, 79.3, and 69.1 ppm represent residues substituted at the C3, C2, C4, and C6 positions, respectively.²⁶ Figure 2a presents the NMR spectrum of heteronuclear multi-quantum coherence (HMQC) for TM3a. This maps the correlation between the directly bonded C and the directly bonded H atoms with distinguishing the protons directly and indirectly linked to a C atom. Figure 2b shows a spectrum of a double-

quantum filter (DQF), indicating the correlation among the H atoms connected within three chemical bonds. The spectra in these two figures allow us to assign the peaks to H and C with the aid of the literature.²⁶ The peaks of the proton at $\delta = 3.12$ to the carbon at $\delta = 77.4$ can be assigned to the pair of H-5/C-5, the protons at $\delta = 3.01$ to the carbon at $\delta = 77.4$ for H-3/C-3, the proton at $\delta = 3.01$ to the carbon at $\delta = 70.6$ for H-4/C-4, and the proton at $\delta = 2.93$ to the carbon at $\delta = 74.1$ for H-2/C-2. Additionally, the absence of OH-1 on the DQF spectra further displays that TM3a is a hyperbranched glucan with numerous terminals being bonded at the C1 position. In view of the NMR results, TM3a is proven as a hyperbranched β -D-glucan mainly containing C3, C2, C4, and C6 substituted residues.

Figure 3 shows the GC-MS profile of methylated TM3a. There are eight components, namely, 2,3,4,6-tetra-*O*-methylglucose, 2,4,6-tri-*O*-methylglucose, 2,3,6-tri-*O*-methylglucose, 2,3,4-tri-*O*-methylglucose, 2,4-di-*O*-methylglucose, 4,6-di-*O*-methylglucose, 2,3-di-*O*-methylglucose, and 1-*O*-methylglucose. This indicates that TM3a consists mainly of terminal glucose, 1,3-linked glucose, 1,4-linked glucose, 1,6-linked glucose, 1,3,6-

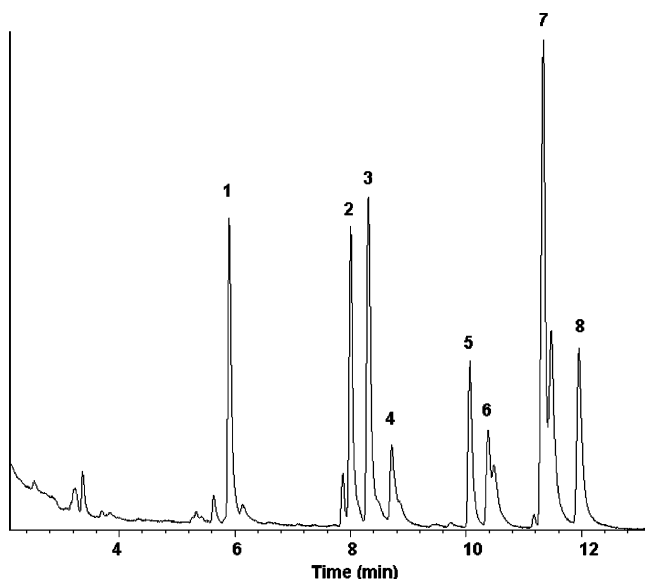


Figure 3. GC profile of methylated TM3a on GC-MS. Signals from 1–8 represent 2,3,4,6-tetra-*O*-methylglucose, 2,4,6-tri-*O*-methylglucose, 2,3,6-tri-*O*-methylglucose, 2,3,4-tri-*O*-methylglucose, 2,4-di-*O*-methylglucose, 4,6-di-*O*-methylglucose, 2,3-di-*O*-methylglucose, and 1-*O*-methylglucose, respectively.

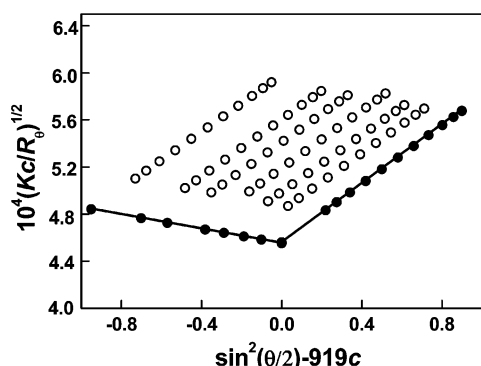


Figure 4. Berry plot for TM3a in 0.25 M LiCl/DMSO at 25 °C.

linked glucose, 1,2,3-linked glucose, 1,4,6-linked glucose, and 2,3,4,6-linked glucose in the molar ratios of 13.0:12.8:16.0:5.7:7.3:3.9:32.3:9.0. The degree of branching (DB) was calculated on the basis of the formula²⁷

$$DB = \frac{N_T + N_B}{N_T + N_B + N_L} \quad (4)$$

where N_T , N_B , and N_L are the total numbers of the terminal residues, branched residues, and linear residues, respectively. According to the analogous method as described in ref 28, the parameters can be obtained from the GC-MS, that is $N_T/N_B/N_L = 13.0:(7.3 + 3.9 + 32.3 + 9.0):(12.8 + 16.0 + 5.7)$. Then, the DB value of TM3a was calculated to be 65.5%.

Fractal Dimension. A good linear relationship between $\eta_{sp}/c - c$ and $(\ln \eta_t)/c - c$ for TM3a fractions has been obtained (not shown). This suggests the exhibition of normal solution behavior. In Figure 4, Berry plots are drawn for TM3a in 0.25 M LiCl/DMSO at 25 °C. As compared to a more familiar Zimm plot, the Berry plot is different with the fact that the root of Kc/R_θ is illustrated, and it also takes into account the influence of a third viral coefficient.²⁹ From the intercept of two straight lines and the slope of angular dependence, the values of M_w and $\langle S^2 \rangle_z^{1/2}$ are estimated, respectively. The angular dependences of $(Kc/R_\theta)^{1/2}_{c=0}$ for the TM3a fractions in 0.25 M LiCl/DMSO

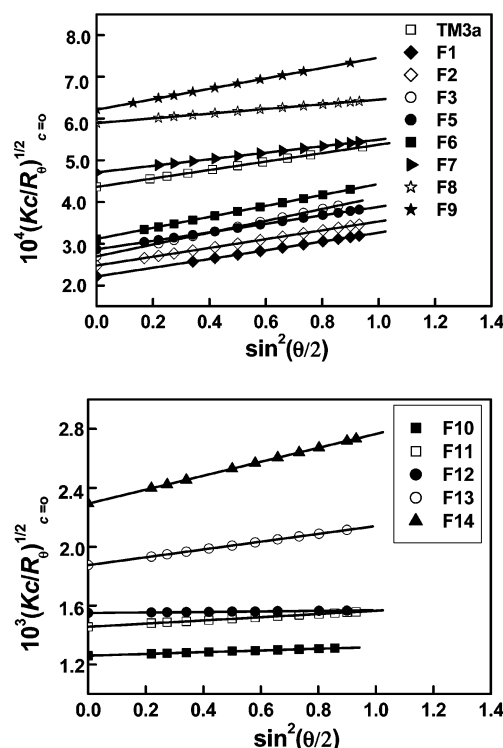


Figure 5. Angular dependences of $(Kc/R_\theta)^{1/2}_{c=0}$ for the TM3a fractions in 0.25 M LiCl/DMSO at 25 °C.

at 25 °C are shown in Figure 5. The experimental results are listed in Table 1. The fractal dimension (d_f) can be used to obtain the relevant structural quantities and further insight into the nature of hyperbranched polysaccharide. For a rigid rod, the value of d_f is 1, and linear polymers with a Gaussian coil nature have a d_f value ranging from 5/3 to 2. A three-dimensional object with a homogeneous density has a mass fractal dimension of 3. The d_f value of monodisperse polymers can be extracted directly from the angular dependence of the scattered light or neutron intensity.³⁰ A scattering factor of a dimensionless particle can be defined for finite concentrations, which is from linear extrapolation to zero concentration of the corresponding data measured in diluted solutions at varying concentrations³¹

$$P_{(q,c=0)} = R_{(\theta,c=0)}/R_{(\theta \rightarrow 0,c=0)} \quad (5)$$

where $R_{(\theta,c=0)}$ is the structure factor and $R_{(\theta \rightarrow 0,c=0)}$ is the corresponding value at scattering angle of $\theta = 0$ (forward scattering). Figure 6 provides the double logarithmic plots of $P_{(q,c=0)}$ against $q\langle S^2 \rangle_z^{1/2}$, where $q\langle S^2 \rangle_z^{1/2}$ is used as a dimensionless length scale. For TM3a fractions, the curves collapsed into one common master curve. The d_f values obtained from the best fit of the corresponding master curve are also listed in Table 1. The values are no longer integers but fractal dimensions, which are common for disordered objects.

The fractal dimensions can also be determined from the relationship between M_w and $\langle S^2 \rangle_z^{1/2}$ and are defined as the inverse of the exponent ν ³²

$$\langle S^2 \rangle_z^{1/2} \sim M^\nu \quad (6)$$

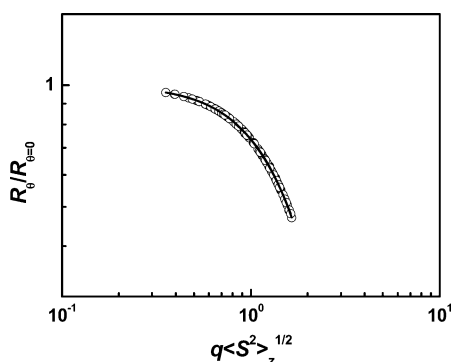
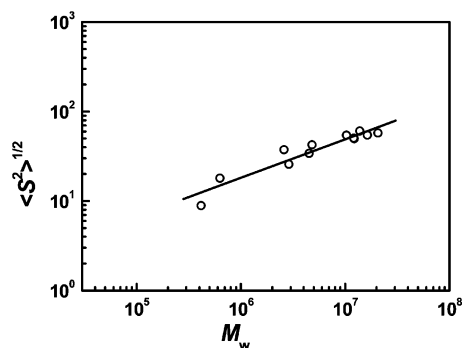
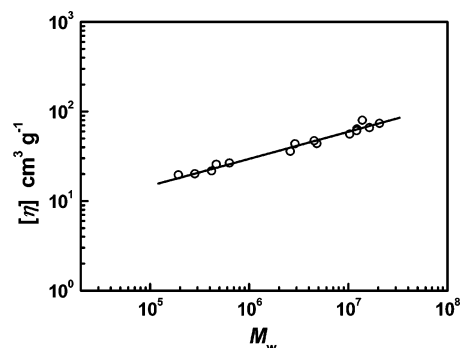
$$d_f = 1/\nu \quad (7)$$

The plot of $\langle S^2 \rangle_z^{1/2}$ versus M_w for the TM3a sample is shown in Figure 7. The resulting relationship is expressed as

$$\langle S^2 \rangle_z^{1/2} = 4.79 \times 10^{-2} M_w^{0.43 \pm 0.04} \text{ (nm)} \quad (8)$$

Table 1. Experimental Results of M_w , $\langle S^2 \rangle_z^{1/2}$, A_2 , d_f , $[\eta]$, R_h , and $(\langle S^2 \rangle_z^{1/2}/R_h)$ for the TM3a Fractions in 0.25 M LiCl/DMSO at 25 °C

sample	$M_w \times 10^{-6}$ (g/mol)	$\langle S^2 \rangle_z^{1/2}$ (nm)	$A_2 \times 10^5$ (mol mL g ⁻²)	d_f	$[\eta]$ (cm ³ g ⁻¹)	R_h (nm)	$\langle S^2 \rangle_z^{1/2}/R_h$
TM3a	4.81	42.5	1.17	2.41	43.8	30.7	1.38
F1	20.6	57.5	0.66	2.20	73.7	41.7	1.38
F2	16.3	54.5	0.63	2.09	66.2	39.9	1.37
F3	13.8	60.6	0.63	2.26	80.0	38.2	1.59
F4	12.2	49.8	0.80	2.09	63.8	38.1	1.31
F5	12.1	50.3	0.82	2.08	61.1	36.9	1.36
F6	10.3	54.3	0.91	2.09	55.9	35.9	1.51
F7	4.51	34.1	1.39	2.15	47.1	26.2	1.30
F8	2.89	25.8	1.85	2.28	43.7	21.7	1.19
F9	2.59	37.4	2.08	2.06	36.0	22.1	1.69
F10	0.63	18.0	6.42		26.6	11.9	1.51
F11	0.46	22.9	28.4		25.7	8.4	
F12	0.42	8.9	5.2		21.7	11.2	0.79
F13	0.28		8.0		20.2	8.0	
F14	0.19		12.5		19.6	7.1	

**Figure 6.** $P_{(q,c=0)}$ as a function of $q\langle S^2 \rangle_z^{1/2}$ for the TM3a fractions in 0.25 M LiCl/DMSO at 25 °C.**Figure 7.** Plot of $\log \langle S^2 \rangle_z^{1/2}$ vs $\log M_w$ for TM3a in 0.25 M LiCl/DMSO at 25 °C.**Figure 8.** $[\eta]$ dependences on the M_w for TM3a in 0.25 M LiCl/DMSO at 25 °C.

On the basis of the theory of polymer solution, the exponent (ν) values of 0.33, 0.50 to 0.6, and 1.0 reflect the chain shape in adapting sphere, random coil, and rigid rod, respectively. The

ν value of 0.43 suggests that TM3a molecules are present between the state of hard sphere and random coil. The d_f value was calculated to be 2.32 for TM3a according to eq 7. The value of 2.32 is characteristic of a particle having an internal structure between the hard sphere ($d_f = 3.0$) and the fully swollen branched macromolecule in a thermodynamically good solvent ($d_f = 2.0$).³² Scherrenberg and co-workers³³ have found that the value of d_f for some dendrimers is 3.

In addition, the d_f value of polymers can also be derived from the Mark–Houwink equation³⁴

$$d_f = 3/(1 + \alpha) \quad (9)$$

where α is the exponent of the Mark–Houwink equation. Figure 8 shows the plot of $[\eta]$ versus M_w for TM3a in 0.25 M LiCl/DMSO at 25 °C. The Mark–Houwink equation of TM3a in the M_w range from 1.94×10^5 to 2.06×10^7 is established as

$$[\eta] = 0.46M_w^{0.30 \pm 0.01} \text{ (cm}^3 \text{ g}^{-1}) \quad (10)$$

The exponent (α) is usually related to the shape of the macromolecule and the nature of the solvent. In general, α with a rough value of 0.5 suggests that the polymer molecules behave as a dense sphere, and the value from 0.6 to 0.8 indicates the existence of a flexible chain and a greater value than one for an elongated rod. The experimental result of 0.30 for TM3a is noticeably low, which is ascribed to a compact sphere-like structure of hyperbranched polymers. If the structure of a polymer chain is a perfect hard sphere, the exponent should be 0 theoretically.³⁵ The value of α depends on the DB as well. The exponents of the Mark–Houwink equation typically vary between 0.34 and 0.20 for hyperbranched glycopolymers at different DB values.³⁶ Therefore, the exponent of the Mark–Houwink equation of TM3a lies in the range for hyperbranched polymers. The d_f value of TM3a was 2.31 by the calculation according to eq 9. The result is in good agreement with that from the measurements of $\langle S^2 \rangle_z^{1/2}$. The fractal dimension is a measurement of the compactness of polymer chains. The larger the value of the fractal dimension, the more compact the polymer structure tends to be. Our result further confirms that the water-insoluble hyperbranched β -glucan exists as a compact chain conformation of sphere-like structure in 0.25 M LiCl/DMSO solution.

Molecular Parameters. The hydrodynamic radius (R_h) can be obtained from the measurement of dynamic light scattering. The R_h values are also summarized in Table 1. The plot of R_h versus M_w for the TM3a fractions in 0.25 M

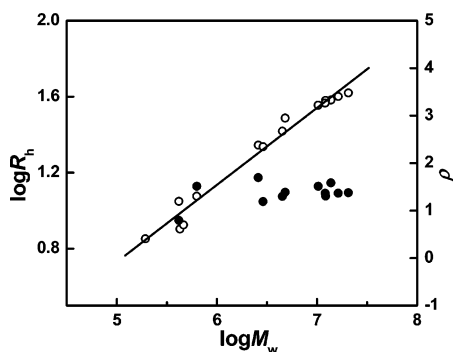


Figure 9. Hydrodynamic radius (○) and ρ (●) as a function of M_w for the TM3a fractions in 0.25 M LiCl/DMSO at 25 °C.

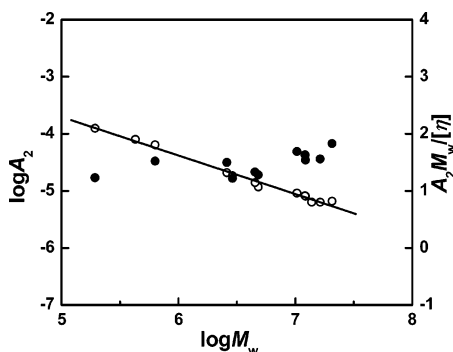


Figure 10. Dependence of A_2 (○) and $M_w A_2 / [\eta]$ (●) on the M_w for the TM3a fractions in 0.25 M LiCl/DMSO at 25 °C.

LiCl/DMSO is shown in Figure 9. The scaling law is represented as

$$R_h = 5.01 \times 10^{-2} M_w^{0.41 \pm 0.02} \quad (11)$$

As is well-known, molecular parameters and dilute solution properties can be gained from their $\langle S^2 \rangle_z^{1/2}$ and R_h values for linear polymers,^{37,38} hyperbranched polymers,³⁹ dendrimers,⁴⁰ and dendrimer-like synthetic polymers.⁴¹ In a given polymer solution, the ratio of geometric to hydrodynamic radius ($\rho = \langle S^2 \rangle_z^{1/2} / R_h$) depends on its chain architecture and conformation. Many previous experimental results have verified the ρ value in the range of 1.5–1.7 for flexible linear polymers in a good solvent,³⁷ whereas the value is 0.78 for a homogeneous sphere. Ratio data of $\langle S^2 \rangle_z^{1/2}$ to R_h are also summarized in Table 1. Figure 9 also shows the plot of the ρ value versus M_w . It is obvious that the ρ value is independent of M_w and has an average value of 1.30. On the basis of a Kirkwood approximation for the hydrodynamic interaction,⁴² the ρ parameter for hyperbranched structures is theoretically predicted as 1.22. It is noted that the mean value of ρ is very close to that of the hyperbranched polymers, implying that TM3a could have a highly branched structure.

The second virial coefficient (A_2) of polymers is another property that is sensitive to the change of branching architecture. Generally, A_2 values of a linear polymer exhibit a M_w dependence over the range of a negative exponent between -0.2 and -0.3 at a good solvent limit. Figure 10 describes M_w dependence on A_2 , and their relationship is represented by

$$A_2 = 0.47 M_w^{-0.68 \pm 0.02} \quad (12)$$

The relatively larger value of a negative exponent (-0.68) is a characteristic of branched structures as compared to that of linear polymers.²⁹ As seen in the expansion $\Pi / (N_A k_B T) = (c/M)[1 +$

$A_2 M c + A_3 M c^2 + \dots]$, the magnitude of $A_2 M c$ tells how much the thermodynamics of a solution is derived from that of the ideal solution. A solution with a greater $A_2 M$ value will develop a nonideality at a lower mass concentration. It is then natural to expect because then

$$A_2 M \cong \frac{1}{c^*} \quad (13)$$

$$c^*[\eta] = 1 \text{ and } [\eta] \propto M^\alpha \quad (14)$$

$$A_2 \propto M^{(\alpha-1)} \quad (15)$$

with the equation of $[\eta] = 0.46 M_w^{0.30 \pm 0.01}$, we obtained $A_2 \propto M_w^{-0.70}$.

Another quantitative definition of c^* is usually used for a branched polymer, star polymer, and spherical polymer because

$$c^* \left(\frac{4\pi}{3} \langle S^2 \rangle_z^{3/2} \right) = \frac{M}{N_A} \quad (16)$$

$$\langle S^2 \rangle_z^{1/2} \sim M^\nu \quad (17)$$

then

$$A_2 \cong \left(\frac{4\pi}{3} \langle S^2 \rangle_z^{3/2} \right) / (M^2 / N_A) \propto M^{(3\nu-2)} \quad (18)$$

with the equation of $\langle S^2 \rangle_z^{1/2} = 4.79 \times 10^{-2} M_w^{0.43 \pm 0.04}$, the relationship of $A_2 \propto M_w^{-0.71}$ was obtained. The calculated exponent values of -0.70 and -0.71 are in good agreement with the exponent value of -0.68 extracted from experiment data of A_2 and M_w . This provides another support for TM3a having a branched architecture.

The relationship of a second virial coefficient against chain dimension relationships is expressed in terms of the penetration function, ψ ⁴³

$$\psi = A_2 M^2 / (4\pi^{3/2} N_A \langle S^2 \rangle_z^{3/2}) \quad (19)$$

The penetration function describes the penetration of hydrodynamic volume from two connected polymer segments.⁴⁴ The formula of intrinsic viscosity versus chain dimension is present in terms of the Flory coefficient, Φ ⁴²

$$\Phi = \frac{[\eta] M_w}{(6 \langle S^2 \rangle_z^{3/2})} \quad (20)$$

The Flory coefficient describes the penetration of the hydrodynamic volume of the polymer by solvent molecules. Furthermore, the relationship between intrinsic viscosity and second virial coefficient relationships can be described in terms of Φ ⁴⁵

$$\sigma = \frac{A_2 M_w}{[\eta]} \quad (21)$$

According to eqs 19–21, we can obtain the σ value by

$$\sigma = \frac{4\pi^{3/2} N_A \langle S^2 \rangle_z^{3/2} / M_w \psi}{\Phi \langle S^2 \rangle_z^{3/2} / M_w} = 4\pi^{3/2} N_A \frac{\psi}{\Phi} \quad (22)$$

where ψ is the coil to coil interpenetration function, and Φ is the solvent to coil penetration function. The ratio of the two values can be used to compare the coil to coil interaction with the hydrodynamic interaction among particles. According to

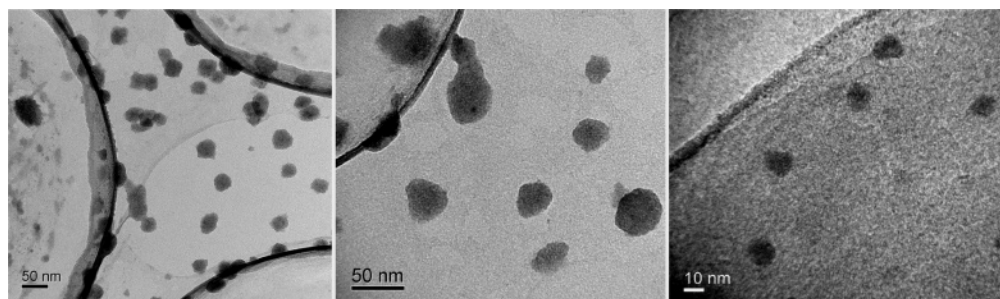


Figure 11. TEM images of TM3a in 0.25 M LiCl/DMSO.

Bauer and Burchard's interpretation, $M_w A_2/[\eta]$ is the ratio of two differently defined volumes of macromolecules in the solution. It can be used in the same manner as the ρ parameter to detect the branching of polymers.⁴⁶ Another approach to understand structural change is the dependence of $M_w A_2/[\eta]$ on M_w . Figure 10 also shows the ratio of $M_w A_2/[\eta]$ as a function of M_w for the TM3a fractions. The result demonstrates that $M_w A_2/[\eta]$ is independent of M_w , and its average value is 1.46. An asymptotic constant value (σ_{line}) of 1.07 ± 0.03 is found for linear flexible chains. The $M_w A_2/[\eta]$ values in some experimental findings are obtained in the range of 2.0–2.4 for the branched structure.³⁴ It is noted that the $M_w A_2/[\eta]$ value decreases to 1.60 for a hard sphere. The smooth and well-defined surface of a hard sphere structure may play a noncomparable effect on hydrodynamic reactions.⁴⁷ The hyperbranched polymer has the difficulty of interpenetration through segment clouds, which become dominant at high M_w . However, the smaller solvent molecules are easy to penetrate the volume pervaded by the hyperbranched macromolecules. Therefore, the value of $M_w A_2/[\eta] = 1.46$ for TM3a reflects that the highly branched polysaccharide intends to form a sphere-like structure.

Molecular Morphology. TEM technology is widely used to observe and measure the morphology and dimension of particles including macromolecules. Figure 11 illustrates the TEM images of TM3a in 0.25 M LiCl/DMSO. The spherical particles of TM3a at the molecular level are dispersed well in the dilute solution. It further confirms that the TM3a molecules exhibit a globular molecular structure. On the basis of the statistic analysis, the average diameter is about 23.0 ± 1.8 nm determined from 125 measurements. The molecular weight of globular molecules can be calculated by

$$M = (4/3)\pi R^3 \rho_p N_A \quad (23)$$

where R is the radius of the particle and ρ_p is the density of polysaccharide. It has been reported that the ρ_p value for amylopectin, a hyperbranched starch from Waxy, falls in the range of 1.48–1.50 g/mL.⁴⁸ By using $\rho_p = 1.49$ g/mL, the M value of TM3a was 5.71×10^6 by the calculation according to eq 23. It is close to that obtained from LLS (4.81×10^6). The result from TEM measurements demonstrates that the individual molecules of TM3a exist as a sphere-like conformation. This is in accordance with that obtained from the theory of polymer solution. Our results prove that the current theory of polymer solution can be used to calculate the conformation parameters of complex hyperbranched polysaccharides in the solution state.

Conclusion

A water-insoluble β -D-glucan, extracted from the sclerotia of *Pleurotus tuber-regium*, was determined as a hyperbranched polysaccharide. According to the current theory of polymer

solutions, the various scaling laws and molecular parameters of polysaccharide were calculated successfully from the experimental data of M_w , $\langle S^2 \rangle_z^{1/2}$, A_2 , R_h , and $[\eta]$. The results revealed that TM3a in LiCl/DMSO at 25 °C was present in a sphere-like conformation as a result of the highly branched structure. In view of the fractal dimension, TM3a in the LiCl/DMSO system had an internal structure between a hard sphere and a swollen branched macromolecule. Furthermore, the TEM images confirmed directly that TM3a molecules existed in a spherical conformation. Therefore, the current theory of polymer solution could be well-applied to analyze the molecular parameters and solution properties of a sophisticated and natural hyperbranched polysaccharide.

Acknowledgment. This work was supported by grant from the National Natural Science Foundation of China (30530850) and the High-Technology Research and Development Program of China (2006AA02Z102).

References and Notes

- Kolender, A. A.; Matulewicz, M. C. *Carbohydr. Res.* **2002**, 337, 57.
- Riccio, R.; Kinnel, R. B.; Bifulco, G.; Scheuer, P. J. *Tetrahedron. Lett.* **1996**, 37, 1979.
- Zhang L., Yang L. *Biopolymers* **1995**, 36, 695.
- Zhang, L.; Zhang, X.; Zhou, Q.; Zhang, P.; Li, X. *Polym. J.* **2001**, 33, 317.
- Zhang, L.; Ding, Q.; Meng, D. Y.; Ren, L. W.; Yang, G.; Liu, Y. G. *J. Chromatogr., A* **1999**, 839, 49.
- Ohno, N.; Miura, N. N.; Chiba, N.; Adachi, Y.; Yadomae, T. *Biol. Pharm. Bull.* **1995**, 18, 1242.
- Zhang, L.; Li, X.; Xu, X.; Zeng, F. *Carbohydr. Res.* **2005**, 340, 1515.
- Scott, R. W. J.; Ye, H.; Henriquez, R. R.; Crooks, R. M. *Chem. Mater.* **2003**, 15, 3873.
- Hecht, S. J. *Polym. Sci., Part A: Polym. Chem.* **2003**, 41, 1047.
- Stiriba, S. E.; Frey, H.; Haag, R. *Angew. Chem., Int. Ed.* **2002**, 41, 1329.
- Satoh, T.; Imai, T.; Ishihara, H.; Maeda, T.; Kitajyo, Y.; Narumi, A.; Kaga, H.; Kaneko, N.; Kakuchi, T. *Macromolecules* **2003**, 36, 6364.
- Luca, E. D.; Richards, R. W. *J. Polym. Sci., Part B: Polym. Phys.* **2003**, 41, 1339.
- Rubio, A. M.; Freire, J. J. *Macromolecules* **1996**, 29, 6946.
- Ourdouillie, P.; Chaumont, P.; Mechin, F.; Dumon, M.; Durand, D.; Nicolai, T. *Macromolecules* **2001**, 34, 4109.
- Motawia, M. S.; Damager, I.; Olsen, C. E.; Møller, B. L.; Engelsen, S. B.; Hansen, S.; Øgendal, L. H.; Bauer, R. *Biomacromolecules* **2005**, 6, 143.
- Imai, T.; Satoh, T.; Kaga, H.; Kaneko, N.; Kakuchi, T. *Macromolecules* **2003**, 36, 6359.
- Zhang, X.; Xu, J.; Zhang, L. *Biopolymers* **2005**, 78, 187.
- Xu, X.; Zhang, X.; Zhang, L.; Wu, C. *Biomacromolecules* **2004**, 5, 1893.
- Cao, X.; Zhang, L. *Biomacromolecules* **2005**, 6, 671.
- Zoberi, M. H. *Nigerian Field* **1973**, 38, 81.
- Oso, B. *Mycologia* **1977**, 69, 271.
- Needs, P. W.; Selvendran, R. R. *Carbohydr. Res.* **1993**, 245, 1.
- Kiho, T.; Sakushima, M.; Wang, S.; Nagai, K.; Ukai, S. *Chem. Pharm. Bull.* **1991**, 39, 798.
- Bock, K.; Pedersen, C. *Adv. Carbohydr. Chem. Biochem.*; Academic press: New York, **1983**, 41, 27.

- (25) Satoh, T.; Imai, T.; Ishihara, H.; Maeda, T.; Kitajyo, Y.; Sakai, Y.; Kaga, H.; Kaneko, N.; Ishii, F.; Kakuchi, T. *Macromolecules* **2005**, *38*, 4202.
- (26) Gorin, P. A. J. *Advances in Carbohydrate Chemistry and Biochemistry*; Academic Press: New York, 1981; Vol. 38, p 13.
- (27) Hawker, C. J.; Lee, R.; Frechet, J. M. J. *J. Am. Chem. Soc.* **1991**, *113*, 4583.
- (28) Bolton, D. H.; Wooley, K. *Macromolecules* **1997**, *30*, 1890.
- (29) Ioan, C. E.; Aberle, T.; Burchard, W. *Macromolecules* **1999**, *32*, 7444.
- (30) Geladé, E.; Goderis, B.; Koster, C.; Meijerink, N.; Benthem, R.; Fokkens, R.; Nibbering, N. *Macromolecules* **2001**, *34*, 3552.
- (31) Cao, X.; Sessa, D. J.; Wolf, W. J.; Willett, J. L. *Macromolecules* **2000**, *33*, 3314.
- (32) Hanselmann, R.; Burchard, W.; Ehrat, M.; Widmer, H. M. *Macromolecules* **1996**, *29*, 3277.
- (33) Scherrenberg, R.; Coussens, B.; Van, V. P.; Edouard, G.; Brockman, J.; De Brabander, E. *Macromolecules* **1998**, *31*, 456.
- (34) Burchard, W. *Adv. Polym. Sci.* **1999**, *143*, 113.
- (35) Park, I. H.; Choi, E. J. *Polymer* **1996**, *37*, 313.
- (36) Muthukrishnan, S.; Mori, H.; Müller, A. H. E. *Macromolecules* **2005**, *38*, 3108.
- (37) Park, S.; Chang, T.; Park, I. H. *Macromolecules* **1991**, *24*, 5729.
- (38) Mays, J. W.; Nan, S.; Lewis, M. E. *Macromolecules* **1991**, *24*, 4857.
- (39) Douglas, J. F.; Roovers, J.; Freed, K. F. *Macromolecules* **1990**, *23*, 4168.
- (40) Striegel, A. M.; Plattner, R. D.; Willett, J. L. *Anal. Chem.* **1999**, *71*, 978.
- (41) Lepoittevin, B.; Matmour, R.; Francis, R.; Taton, D.; Gnanou, Y. *Macromolecules* **2005**, *38*, 3120.
- (42) Burchard, W.; Schmidt, M.; Stockmayer, W. H. *Macromolecules* **1980**, *13*, 1265.
- (43) Yamakawa, H. *Modern Theory of Polymer Solutions*; Harper and Row: New York, 1971.
- (44) Striegel, A. M. *Polym. Int.* **2004**, *53*, 1806.
- (45) Davidson, N. S.; Fetters, L. J.; Funk, W. G.; Graessley, W. W.; Hadjichristidis, N. *Macromolecules* **1988**, *21*, 112.
- (46) Bauer, J.; Burchard, W. *Macromolecules* **1993**, *26*, 3103.
- (47) Gabriela, G.; Burchard, W. *Macromolecules* **1996**, *29*, 1498.
- (48) Zhao, W. B. *Polymer Data Handbook*; Oxford University Press, Inc.: Oxford, 1999; p 975.

BM070335+